Geoscience Frontiers 4 (2013) 623–632

Contents lists available at SciVerse ScienceDirect

China University of Geosciences (Beijing)

Geoscience Frontiers

journal homepage: www.elsevier.com/locate/gsf

Research paper

Last deglacial relative sea level variations in Antarctica derived from glacial isostatic adjustment modelling

Jun'ichi Okuno [a,b,*], Hideki Miura [a,1]

[a] National Institute of Polar Research, 10-3 Midori-cho, Tachikawa, Tokyo 190-8518, Japan
[b] Research Institute for Global Change, Japan Agency for Marine-Earth Science and Technology, 3173-25 Showa-machi, Kanazawa-ku, Yokohama 236-0001, Japan

ARTICLE INFO

Article history:
Received 18 June 2012
Received in revised form
13 November 2012
Accepted 23 November 2012
Available online 16 December 2012

Keywords:
Antarctic ice sheet
Relative sea level
Glacial isostatic adjustment
Melting history
Lithospheric thickness

ABSTRACT

We present relative sea level (RSL) curves in Antarctica derived from glacial isostatic adjustment (GIA) predictions based on the melting scenarios of the Antarctic ice sheet since the Last Glacial Maximum (LGM) given in previous works. Simultaneously, Holocene-age RSL observations obtained at the raised beaches along the coast of Antarctica are shown to be in agreement with the GIA predictions. The differences from previously published ice-loading models regarding the spatial distribution and total mass change of the melted ice are significant. These models were also derived from GIA modelling; the variations can be attributed to the lack of geological and geographical evidence regarding the history of crustal movement due to ice sheet evolution. Next, we summarise the previously published ice load models and demonstrate the RSL curves based on combinations of different ice and earth models. The RSL curves calculated by GIA models indicate that the model dependence of both the ice and earth models is significantly large at several sites where RSL observations were obtained. In particular, GIA predictions based on the thin lithospheric thickness show the spatial distributions that are dependent on the melted ice thickness at each sites. These characteristics result from the short-wavelength deformation of the Earth. However, our predictions strongly suggest that it is possible to find the average ice model despite the use of the different models of lithospheric thickness. By sea level and crustal movement observations, we can deduce the geometry of the post-LGM ice sheets in detail and remove the GIA contribution from the crustal deformation and gravity change observed by space geodetic techniques, such as GPS and GRACE, for the estimation of the Antarctic ice mass change associated with recent global warming.

1. Introduction

An important source of information on the ice thicknesses and extents since the Last Glacial Maximum (LGM) is the changes in the relative sea level (RSL). In regions where high-quality RSL data are available, these data can be used to constrain past ice sheet changes (e.g., Zwartz et al., 1998), mantle viscosity (e.g., Nakada and Lambeck, 1989), or both. In Antarctica, however, there are few geological and geographical RSL observations, largely due to the lack of coastal ice-free areas where organic material for radiocarbon dating can accumulate. Thus, RSL curves have been obtained at a small number of sites on the Antarctic Peninsula (Bentley et al., 2005); on the coast of East Antarctica in the Vestfold Hills (Zwartz et al., 1998), Sôya Coast (Miura et al., 2002) and Windmill Islands (Goodwin, 1993); and in the Ross Sea region (Baroni and Hall, 2004). Nakada et al. (2000) demonstrated RSL variations along the coast of Antarctica from glacial isostatic adjustment (GIA) modelling and constrained the maximum (ANT5) and minimum (ANT6) models of the ice-loading histories of the Antarctic ice sheet during the last deglaciation by comparing the modelling results and field observations. Furthermore, Ivins and James (2005) improved the reconstruction of the Antarctic ice sheet history using both RSL data and space-based geodetic observations (GPS and GRACE) and proposed a new ice load model (IJ05) that is consistent with both the geologic and geodetic observations in Antarctica.

* Corresponding author. National Institute of Polar Research, 10-3 Midori-cho, Tachikawa, Tokyo 190-8518, Japan. Tel.: +81 45 778 5622.
E-mail addresses: okuno@jamstec.go.jp (J. Okuno), miura@nipr.ac.jp (H. Miura).
[1] Tel.: +81 42 512 0703.

Peer-review under responsibility of China University of Geosciences (Beijing).

Production and hosting by Elsevier

1674-9871/$ – see front matter © 2012, China University of Geosciences (Beijing) and Peking University. Production and hosting by Elsevier B.V. All rights reserved.
http://dx.doi.org/10.1016/j.gsf.2012.11.004

Far-field sea level observations from Barbados, the Sunda shelf and Tahiti (Fairbanks, 1989; Hanebuth et al., 2000; Deschamps et al., 2012) show a large and rapid rise in sea level approximately 14 calibrated kilo-years before present (cal. kyr BP). This event, described as meltwater pulse IA (MWP-IA), is considered to represent a eustatic sea level (ESL) rise of approximately 20 m over 500 yr. Clark et al. (2002) suggested that the Antarctic ice sheet melting contributed to the MWP-IA event, and the results contribute to the controversy regarding whether the MWP-IA event was sourced primarily from the northern or southern hemisphere (Clark et al., 2002; Bassett et al., 2005; Peltier, 2005). Recently, Bassett et al. (2005) extended the work of Clark et al. (2002) to consider the full viscoelastic solid earth response to MWP-IA. Comparing the GIA modelling and far-field observations from Tahiti, Barbados and Sunda indicated that a dominant Antarctic contribution to MWP-IA (ca. 15 m eustatic equivalent) is required to fit the far-field observations with a single ice history and earth model. Accordingly, the estimation of the Antarctic ice sheet history during the last deglaciation provides an important clue to understand the mechanism of the abrupt climate change.

In this study, we present the RSL predictions along the coast of Antarctica using the typical ice-loading models and earth structure models, which are characterised by the lithospheric thickness (effective elastic thickness: T_e), to validate the permissible combinations of conventional ice and earth models.

2. Glacial isostatic adjustment modelling

2.1. Sea level equation

Sea level variations predicted by the GIA modelling associated with the last deglaciation on a viscoelastic Earth have been formulated by Farrell and Clark (1976). The RSL variation ($\Delta\zeta_{RSL}$) at site x and time t can be expressed as follows (e.g., Farrell and Clark, 1976; Nakada and Lambeck, 1987):

$$\Delta\zeta_{RSL}(x,\ t) = \Delta\zeta_{ESL}(t) + \Delta\zeta_{isos}(x,\ t) + \Delta\zeta_{local}(x,\ t) \quad (1)$$

in Eq. (1), $\Delta\zeta_{RSL}$ represents a change in sea level relative to the present sea level. RSL changes vary both over time (t) and in space (x), and their causes may be divided into three distinct terms. ESL change ($\Delta\zeta_{ESL}$) is the spatially uniform change in sea level that occurs when a volume of water is released from the ice sheets into the ocean. Sea level change induced by isostatic crustal deformation ($\Delta\zeta_{isos}$) varies in both space and time and is the result of perturbations to the shape of the solid Earth and the geoid due to temporal variation in the loading by ice and water. These two components represent the changes in sea level that result from GIA. The third term ($\Delta\zeta_{local}$) in Eq. (1) refers to the local factors that cause sea level change. This term includes the local tidal regime, the consolidation of sediments and tectonic processes. These factors are neglected in this paper, as their contributions to the sea level in the region where we focused are relatively small.

Several important processes are neglected in the original formulation of the sea level equation defined by Farrell and Clark (1976). These processes have been progressively included in subsequent GIA studies. The treatment of shoreline migration, the presence of grounded or floating ice and rotational feedback within the sea level equation are described below.

The first studies to implement time-varying ocean geometry in the context of GIA were performed by Lambeck and Nakada (1990) and Johnston (1993). Subsequent studies have developed increasingly accurate techniques to address shoreline migration (e.g., Milne et al., 1999; Okuno and Nakada, 2001; Lambeck et al., 2003; Mitrovica and Milne, 2003). It has become standard practice to use a time-varying version of the ocean function to obtain precise solutions of the sea level equation. In particular, the evaluation of an ocean function is very important in calculating the sea level changes for the former glaciated regions characterised by both large crustal deformations due to glacial rebound and the existence of ice sheets (e.g., Milne et al., 1999; Okuno and Nakada, 2001). We use a formulation of the water load component introduced by Milne et al. (1999). Milne et al. (1999) used an ocean function based on paleotopography, including the height of the ice sheet, in which they considered the water loads due to the influx of meltwater to subgeoidal solid surface regions previously covered with the marine-based late Pleistocene ice sheets. In fact, the water influx in these regions, including Hudson Bay and the Gulf of Bothnia, contributes significantly to the surface load (e.g., Milne et al., 1999; Okuno and Nakada, 2001).

Further modifications to the extent of the ice- and ocean-loading functions arise in the presence of floating and marine-grounded ice. In previous versions of the sea level equation, ocean-loading has been assumed to be the change in the height of the ocean column. However, in the presence of floating or marine-grounded ice, the water load change will be replaced by the ice load change, and loading at this location will depend upon ice thickness instead of ocean height in the case of floating ice, or only on ice thickness in the case of marine-grounded ice. Special care must be taken when calculating the local changes in RSL following the inundation with water of regions uncovered by retreating marine-grounded ice or the advance of marine-grounded ice into locations with non-zero ocean depth (e.g., Okuno and Nakada, 2002). Ice- and ocean-loading functions must also consider the position of the transition from grounded to floating ice, which is assumed to occur when the mass of the water displaced by the ice is greater than the mass of the ice.

In theory, the sea level equation presented by Farrell and Clark (1976) is based on a non-rotating Earth. Several studies have extended this theory to include rotational effects (e.g., Milne and Mitrovica, 1996, 1998b). Changes in the configuration of the Earth's surface mass load (ice and ocean) perturb the Earth's rotation vector. A change in the rotational state of the Earth deforms both the geoid and the solid surface and hence affects the sea level, thus further reconfiguring the Earth's surface mass load. This feedback process must be incorporated into the sea level equation and will require iterative methods to solve (e.g., Mitrovica et al., 2005).

Neglecting any of the processes described above introduces errors into the GIA calculations. The largest error arises due to the neglect of shoreline migration; the RSL change since the LGM will be over/under-estimated by up to 125 m (i.e., the eustatic change since the LGM) within the region of shoreline migration. Errors of over 10% may also be incurred in regions with broad continental shelves, and late Holocene far-field sea level highstand predictions may contain errors of over 2 m (e.g., Milne and Mitrovica, 1998a; Okuno and Nakada, 1998). The error will be smaller in regions with steep topography at the shoreline, as such topography limits the spatial extent of shoreline migration. The errors can be reduced to approximately 1% using the calculation algorithms developed by Johnston (1993), Milne et al. (1999) and Okuno and Nakada (2001), and will be a function of the time step used.

2.2. Ice histories

In GIA modelling, ice-loading history is defined using temporal step functions; the ice thicknesses at each location are specified at a series of discrete times. The early models used parabolic 'disks' of ice whose thicknesses, but not radius, vary with time. The axisymmetric disks enable the analytical determination of the viscoelastic response to such a load by the spherically symmetric Maxwell Earth (e.g., James and Ivins, 1998 for a thorough analysis). The more recent models specify the ice thicknesses for a given time

at a set of discrete points on the surface of the Earth. The ice thickness distribution is converted into a spherical harmonic loading function (Spada and Stocchi, 2007) when solving the sea level equation using spectral methods (e.g., Nakada and Lambeck, 1987). It is commonly assumed that the ice thickness varies linearly between time steps.

The spatial and temporal variations of ice sheets are very important for calculating RSL variations (e.g., Nakada and Lambeck, 1988). The ice models adopted here are the ARC3 + ANT4 (Nakada and Lambeck, 1989), ARC3 + ANT5 (Nakada et al., 2000), ICE-3G (Tushingham and Peltier, 1991), ICE-5G (Peltier, 2004) and IJ05 (Ivins and James, 2005). The spatial distributions of the total melted ice thickness since the LGM in Antarctica are shown in Fig. 1 for the ANT4, ANT5, ICE-3G, ICE-5G and IJ05 ice models. The ESL curves for these models are shown in Fig. 2. The Antarctic components of ICE-3G, ANT3 and ANT4 are essentially based on the CLIMAP (Denton and Hughes, 1981) reconstruction. These figures indicate that there are large dissimilarities in the spatial, temporal and total amount of melting ice mass among the models. Hence, the details of the Antarctic ice sheet evolution are the subject of debate.

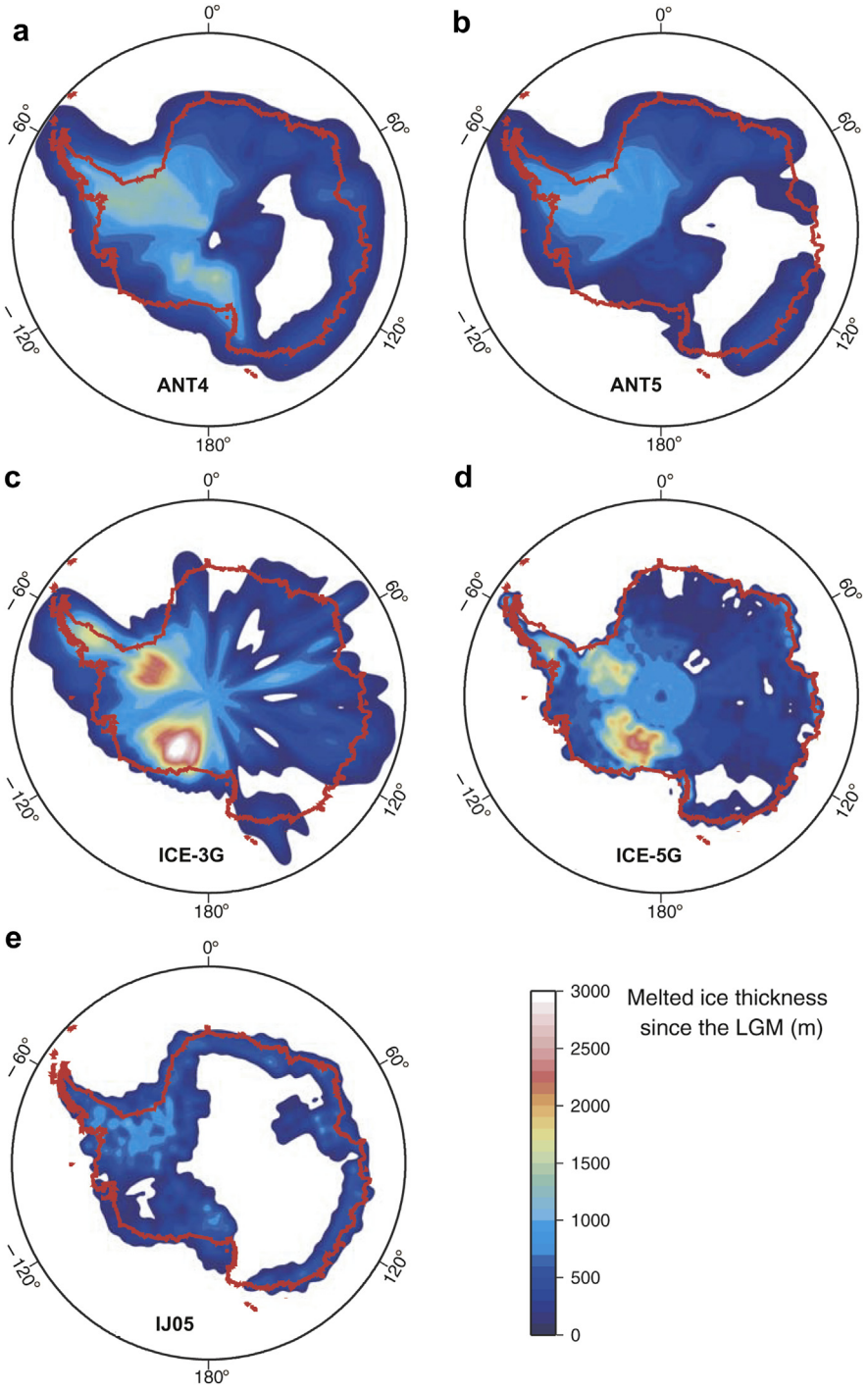

Figure 1. Thicknesses of Antarctic ice melted since the LGM for ANT4, ANT5, and IJ05 and the Antarctic components of ICE-3G and ICE-5G.

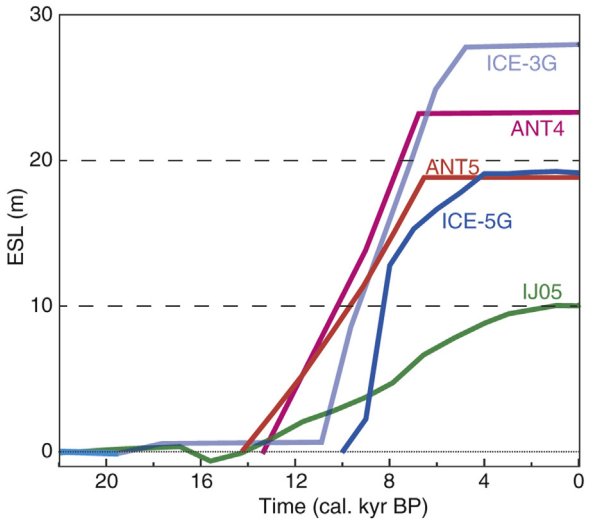

Figure 2. Eustatic sea level curves for ANT4, ANT5, and IJ05 and the Antarctic components of ICE-3G and ICE-5G.

The most widely used global ice models are the ICE-3G (Tushingham and Peltier, 1991) and ICE-5G (Peltier, 2004) models. These models are constrained by geological data and have been developed in conjunction with GIA modelling. ICE-5G is an updated version of ICE-3G, developed following the introduction of improved ice-dynamic modelling and the availability of supplemental data, including geodetic and gravity data from North America (Argus et al., 1999; Lambert et al., 2001) and Greenland. In particular, ICE-5G is used in conjunction with the VM2 Earth model (Peltier, 2004), as shown in Fig. 3b. The measurements of GIA observables in Greenland and Antarctica will contain signals relating to both post-LGM and present-day melting; these signals must be separated to study about the LGM ice configuration (Velicogna and Wahr, 2002; Ivins and James, 2005). The estimates for the global ice volume at LGM range from 43.5 $\times$ 10^6 km^3 to 51 $\times$ 10^6 km^3 (Milne and Mitrovica, 2002), equivalent to an ESL change of 115–135 m. Lambeck et al. (2002) concluded that ice volumes were almost constant between 30 kyr BP and 19 kyr BP, during which time the eustatic sea level was 120–130 m lower than the present level and the global sea level started to rise at 19 kyr BP (Yokoyama et al., 2000).

The GIA models have also been used to reconstruct the rates of ESL change (e.g., Okuno and Nakada, 1999; Lambeck et al., 2002) and to investigate the source of rapid deglacial events such as MWP-1A (e.g., Deschamps et al., 2012). Lambeck et al. (2002) predicted maximum rates of eustatic sea level change of up to 15 mm/yr on either side of the Younger Dryas and suggest that the eustatic sea level stabilised at present-day levels approximately 7 kyr BP. Fig. 2 illustrates the ESL curves of the Antarctic component published in previous works. These models indicate that the onset age of deglaciation is approximately 14–10 cal. kyr BP in almost all models. None of these previous models include the rapid ice melting during the MWP-1A event. The differences in the total melting volumes during the last deglaciation among the models, equivalent to an approximately 10–25 m sea level rise, are significant.

2.3. Viscosity models

The principal aim of many GIA model studies is to constrain mantle viscosities. Many studies invert for earth models of three layers: the lithosphere, upper mantle, and lower mantle (e.g., Lambeck et al., 1998). The solid-earth isostatic component of the sea level signal is computed using the impulse response formalism (Peltier, 1974), which yields the response of a spherically symmetric, self-gravitating and compressible Maxwell viscoelastic earth model to an impulse forcing. The radial elasticity and density structure of the earth model is based on the seismically inferred Preliminary Reference Earth Model (PREM) (Dziewonski and Anderson, 1981). The radial viscosity structure is more crudely parameterised into an upper region of effectively infinite viscosity, simulating an elastic lithosphere, and two deeper regions, each with a uniform viscosity, corresponding to the sub-lithospheric upper mantle and the lower mantle (below a depth of 670 km). In global GIA modelling, the values for the thickness of the lithosphere, which behaves as an elastic layer, lie in the range 50–170 km (Milne and Mitrovica, 1998b). However, recent studies have demonstrated the importance of using a value for the lithospheric thickness that represents the local conditions to accurately fit the data. The regional thicknesses obtained via GIA modelling include 120 km for central Fennoscandia, 60 km for the British Isles and 70 km for the Barents Sea (Steffen and Kaufmann, 2005). Similarly, the upper and lower mantle viscosities cover a range of values. The best-fitting upper mantle viscosities typically lie in the range 10^{20}–10^{21} Pa s, and the lower mantle viscosities lie in the range 5 $\times$ 10^{21}–10^{23} Pa s (e.g., Kaufmann and Lambeck, 2000, 2002; Mitrovica and Forte, 2004). These values have been further refined to fit regional data sets, although some dependence upon the data used has been found. For example, Steffen and Kaufmann (2005) found that an upper mantle viscosity of 4 $\times$ 10^{20} Pa s best fits the Fennoscandian RSL data, whereas a value of 7 $\times$ 10^{20} Pa s best fits the BIFROST GPS data.

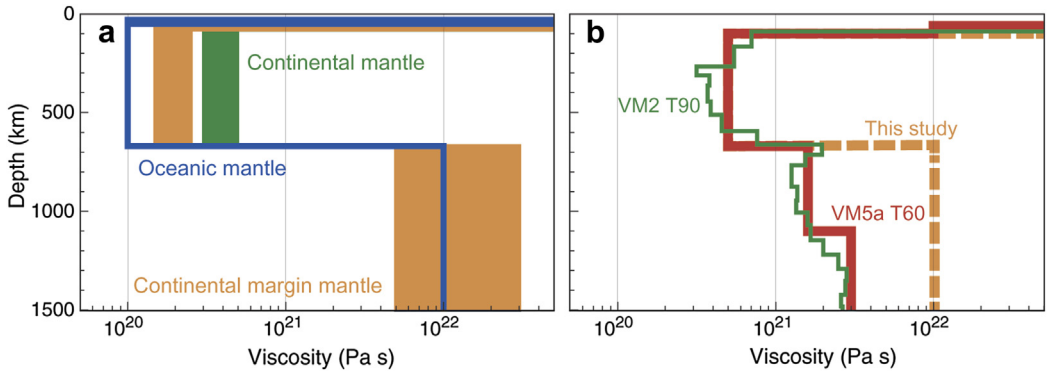

Figure 3. Mantle viscosity structure profiles as a function of depth from Lambeck and Chappell (2001), Peltier (2004), Peltier and Drummond (2008) and Argus and Peltier (2010). The viscosity model used in this study is illustrated in panel (b) by the dashed line. The values of the upper and lower mantle viscosities are 5 $\times$ 10^{20} Pa s and 10^{22} Pa s, respectively.

In Fig. 3, typical mantle viscosity structure models are shown as a function of depth in the ANU group (a) (e.g., Lambeck and Chappell, 2001) and Peltier group (b) models (e.g., Peltier, 2004). The ANU group models were constructed by analysing the RSLs in three different regions. The continental mantle model is based on sea level data in northern Europe (Lambeck et al., 1996, 1998); the continental margin results are based on the late Holocene data from Australia (Nakada and Lambeck, 1989; Lambeck and Nakada, 1990), and the oceanic model is based on the Pacific sea levels (Nakada and Lambeck, 1991). The VM2 T90 (Peltier, 2004) model has a high-viscosity layer (approximately 4×10^{21} Pa s) of approximately 2000 km, and in VM5a T60 (Peltier and Drummond, 2008; Argus and Peltier, 2010), a thin high-viscosity layer (10^{22} Pa s) lies between 60 and 100 km in depth. In this study, we chose 100-km- and 50-km-thick elastic lithospheres and viscosities of 5×10^{20} Pa s for the upper mantle and 10^{22} Pa s for the lower mantle as the standard viscosity model. These parameters are broadly consistent with the results of a number of recent viscosity inferences (Nakada and Lambeck, 1989; Lambeck and Nakada, 1990; Lambeck, 1993; Forte and Mitrovica, 1996; Mitrovica and Forte, 1997; Lambeck et al., 1998; Milne et al., 2001). Recent studies by Whitehouse et al. (2012a, b) investigated the ice extent and GIA models with RSL and GPS-derived uplift data in Antarctica. These studies suggest that the viscosity structure for the whole Antarctica is that lithospheric thickness is 120 km, and upper and lower mantle viscosities are 10^{21} Pa s and 10^{22} Pa s, respectively.

3. Relative sea level observations in Antarctica

Many raised beaches have been investigated in ice-free areas along the coast of Antarctica. Since the coastal regions of Antarctica are uplifting due to the last deglaciation of the Antarctic ice sheet, former shorelines have been recorded in the coastal topography as the ice sheet has retreated. The sea level reconstructions have been derived from the radiocarbon dating of organic material in the raised beaches (penguin remains, shells, seaweed, seal skin). These observations are indicators of past sea levels. We can also reconstruct past sea levels using the sediment cores from isolation basins with a known sill height and dating the transitions from lacustrine to marine and marine to lacustrine sediments. This method has been used to obtain RSL curves for areas covered by ice sheets, such as Greenland (Long and Roberts, 2003) and East Antarctica (Zwartz et al., 1998).

The RSL data sets in this study are from ten locations on the Antarctic continent (Fig. 4) and cover the period of approximately up to 12 cal. kyr BP. The data were compiled by Nakada et al. (2000) and Bassett et al. (2007) and are partially contained in the Antarctic Glaciological Geological Database (http://www.antarctica.ac.uk/met/rcah/agdb/index.htm). The model predictions are generated in cal. kyr BP, and we calibrate the calculated observational ages using the program Calib 6.0 based on INTCAL Marine09 (Reimer et al., 2009) and a ΔR (local reservoir age anomaly) of 1144 ± 120 yr, recently published by Hall et al. (2010). The radiocarbon dating of marine fossils around Antarctica is problematic because of the depletion of ^{14}C that results from dilution with glacier meltwater and the upwelling of deep old ocean water (Omoto, 1983; Stuiver et al., 1986). Hall et al. (2010) have proposed a time-dependent ΔR (the local deviation from the global average) for the past 6000 yr.

4. Numerical results and discussion

Fig. 5 shows the observations and predictions using the earlier models, ANT4 and ICE-3G. The solid red circles represent the mean sea level determined by geographical evidence and fossil ages. The green open and solid circles show the upper and lower bound indicators of past sea levels. We employ two effective elastic thickness (T_e) models: 50 and 100 km. This figure indicates that the predictions based on combinations of deglaciation and T_e models cannot explain the observations at all sites concurrently. In addition, the sensitivity of the RSL prediction to the T_e model depends on the melted ice thickness since the LGM over each site individually. On the other hand, Nakada et al. (2000) examined the sensitivity of the RSL prediction to the viscosity model. In Nakada et al. (2000), RSL predictions were compared based on two rheological models: HVM and UVM. In that calculation, the ice model of ARC3 + ANT4 was employed and T_e for the two rheological models was assumed to be 100 km. The upper and lower mantle viscosities for model HVM are 5×10^{20} and 10^{22} Pa s, and those for model UVM are 10^{21} and 2×10^{21} Pa s respectively. Model HVM, which is same model used in this study, has been supported by sea level studies in the far-field and Fennoscandia areas (e.g., Nakada and Lambeck, 1989; Lambeck et al., 1996). Model UVM has been derived from the analysis of RSL variations in the Laurentide area (e.g., Tushingham and Peltier, 1991). Published results of the comparison between predictions of these viscosity models (Fig. 4 in Nakada et al., 2000) are not particularly sensitive to viscosity structure under the elastic lithosphere. Therefore it is possible to provide the dependences of RSL prediction on the deglaciation model of Antarctic ice sheet and T_e regardless of uncertainties in the viscosity structure beneath the elastic lithosphere. Henceforth, we adopt the viscosity model in which upper and lower mantle viscosities are 5×10^{20} and 10^{22} Pa s, respectively.

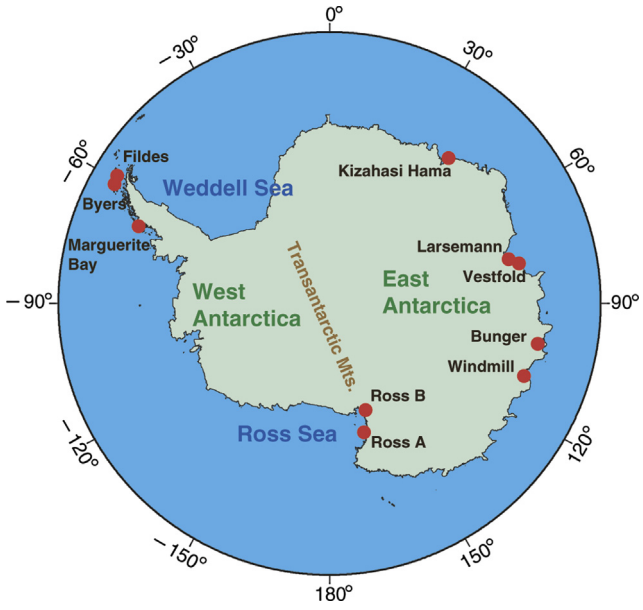

Figure 4. Location map for the data sites used in this study.

Fig. 6 illustrates the RSL curves calculated by ice models published after Nakada et al. (2000). The red, green and blue shaded regions show the calculation range based on the T_e dependence of various ice models. The predicted curves based on ANT5 are indicative of the slight dependence on T_e at almost all sites. These results suppose that the spatial variations of the melted ice thickness of ANT5 are smoother than the variations of ICE-5G, as illustrated in Fig. 1. Previous studies of GIA indicate that near-field RSL predictions are affected by local load history, significantly (e.g., Nakada and Lambeck, 1987). In addition to this, RSL prediction based on the thinner T_e model reflects the short-wavelength load geometry. This is because short-wavelength deformation of the

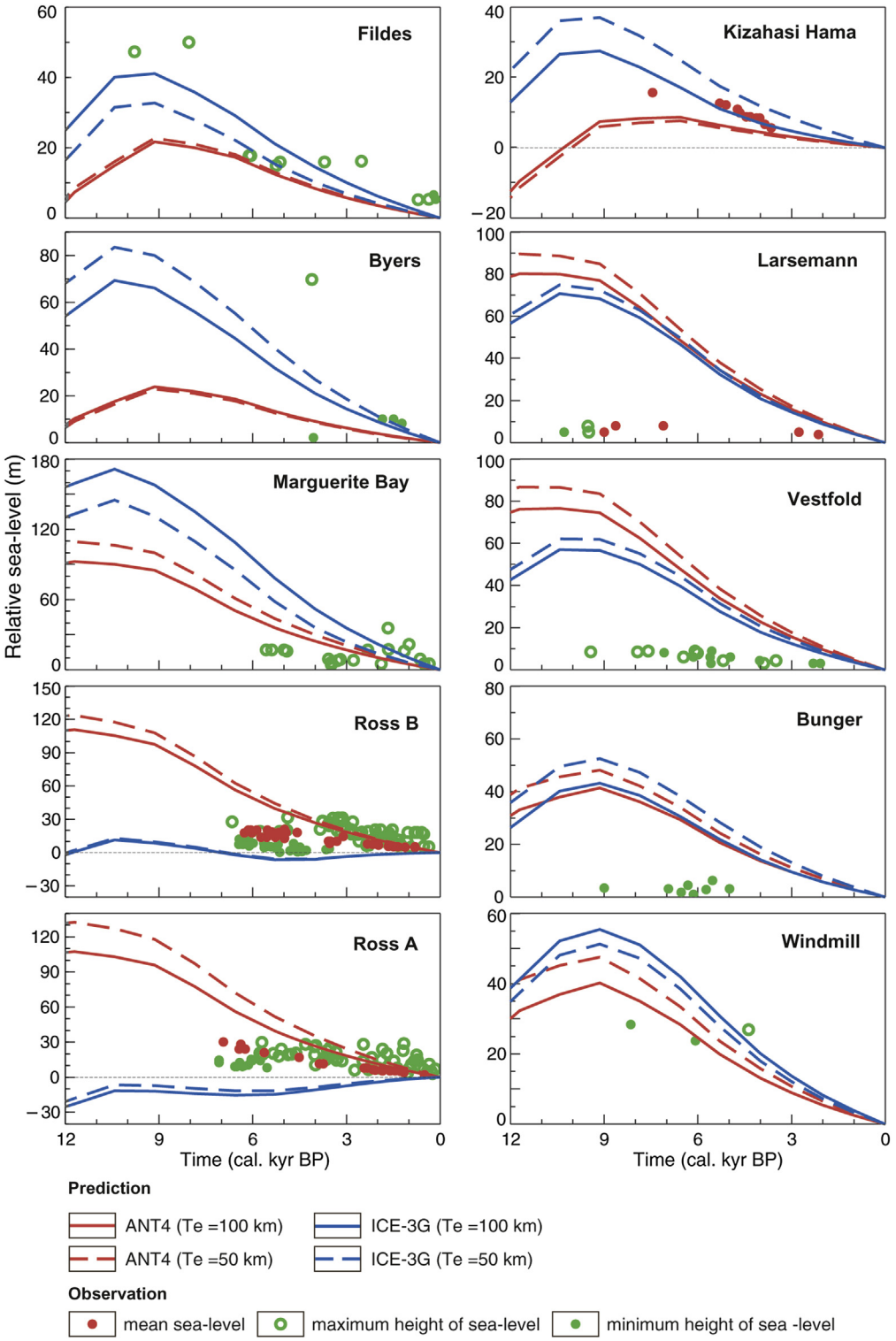

Figure 5. Observed sea level variations and predictions based on the ice models of ANT4 and ICE-3G. The red solid circles represent the past mean sea level determined by organic materials such as fossil shells. The green solid and open circles indicate the upper and lower bounds of the sea level evidence dated by, for example, penguin and elephant seal bone. In these calculations, we employ a viscosity model assuming that the upper and lower mantle viscosities are 5×10^{20} and 10^{22} Pa s, respectively. The lithospheric thickness (effective elastic thickness: T_e) models used here are 100 km and 50 km.

Earth emerges by local load change. There are some sites where the difference between the RSL predictions by the combinations of T_e and deglaciation models is large (e.g., Ross sea region in Fig. 6). These differences are attributed to the difference in the thickness of the melted ice at each sites and in its spatial extent. So the causes of spatial variations of RSL prediction are associated with the spatial variations of earth's deformation. If we adopt the ice model with many small ice-domes in Antarctica, spatial variation of the predicted RSL based on the thinner T_e is characterised by short-wavelength deformation. (e.g., predictions by ICE-5G in Fig. 7). In

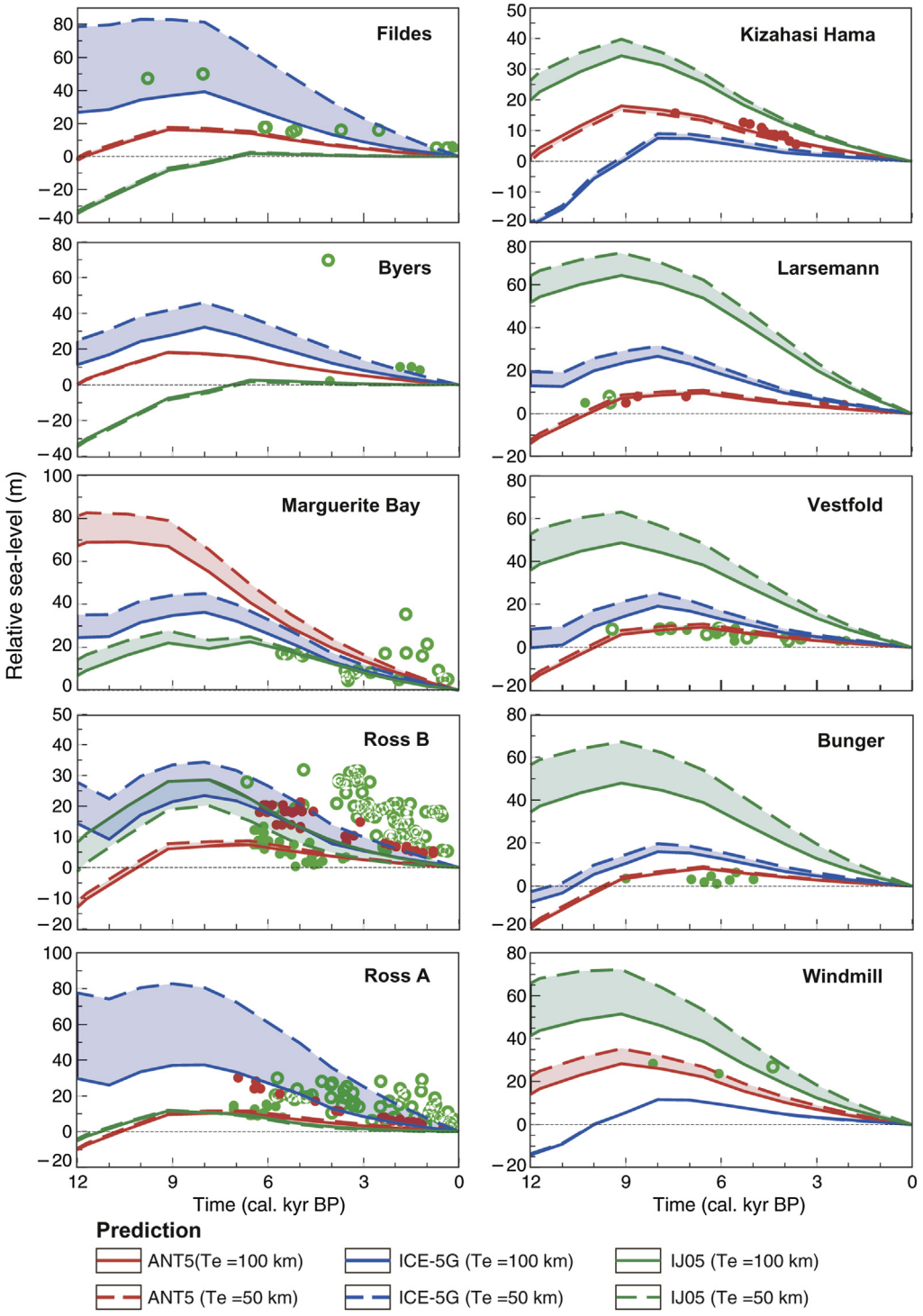

Figure 6. Observed and predicted RSLs at each site in Fig. 3. The ice models used are ANT5, ICE-5G and IJ05. The T_e models used here are 100 km and 50 km. The shaded regions illustrate the range of predictions based on the two T_e models. The symbols are the same as those in Fig. 5.

order to reconstruct an average ice load model by GIA modelling, as much as possible, this should be spatially homogeneous model of melted ice thickness as the surface load change. However, these models do not contain the physical and chemical processes inside the ice sheet, such as thermomechanical ice flow, these uncertainties will remain. In particular, the treatment of ice shelf and the variation in the area of grounded ice are important factors to reconstruct the past ice sheet geometry and thickness (e.g., Saito and Abe-Ouchi, 2010). On the other hand, ice models as the load history inferred from GIA modelling are valuable to examine the present crustal deformation observed by GPS and GRACE. Recently, the construction of the coupled model with bedrock deformation and ice sheet flow is developed, and more realistic models are suggested (e.g., Whitehouse et al., 2012a).

Fig. 7 depicts the spatial distributions of RSL at 7 kyr BP. These results indicate that the spatial variations of RSL depend on the

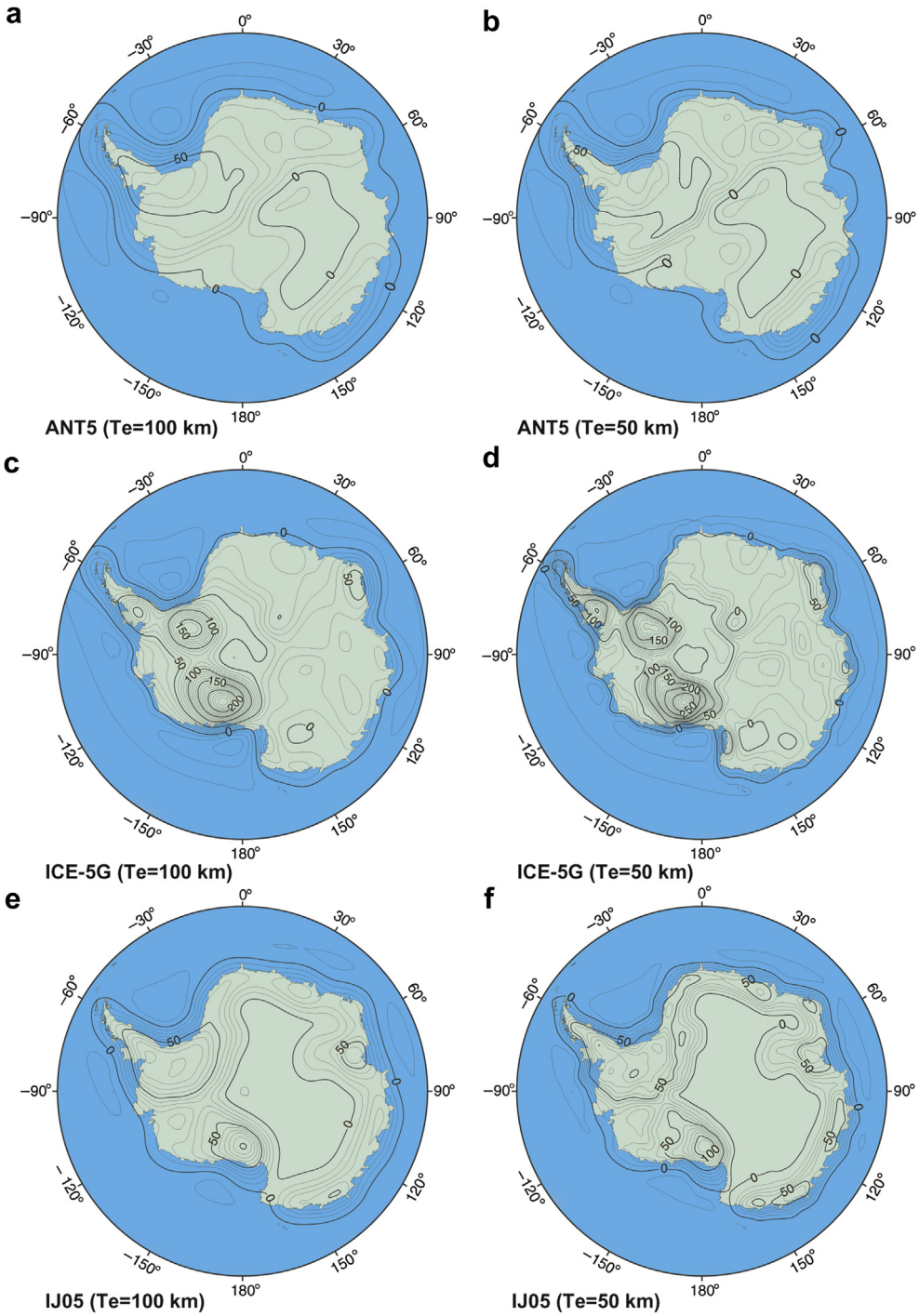

Figure 7. Spatial distributions of RSL at 7 cal. kyr BP for several ice models and for the 100 km and 50 km T_e models.

spatial distribution of melted ice thickness in Fig. 1. In other words, spatial variations of RSL at 7 kyr BP are reflections of ice-sheet models, which ice model dependence seems to be large. This means that the spatial characteristics of predictions are less dependent on earth models. These results suggest that the uncertainties in ice models exceeded the impact of different earth models. In addition, the predictions based on the small value of T_e present a sharp inclination because the short-wavelength deformation caused by a thin elastic layer affects the spatial variations. It is difficult to constrain the melting ice model in the region of inland Antarctica because of the lack of geographical evidence. Only space gravity data are available to constrain the distribution of the past ice sheet geometry (e.g., Ivins and James, 2005). The results of this study clarify that the spatial variations of RSL are sensitive to the choice of the ice and T_e models. The appropriate ice and T_e models can be deduced from future observations, based on comparing the geophysical and geographical signals and the GIA predictions. These results imply the potential to reconstruct the deglaciation history model with less dependence on earth structure using GIA modelling.

5. Summary

We have summarised the RSL predictions based on GIA modelling and the observational evidence of past sea levels in the coastal regions of Antarctica. The results of the theoretical RSL curves and the spatial variations of RSL at 7 kyr BP indicate a significant dependence on the adoption of ice and T_e models. However, the RSL predictions based on ANT5 and IJ05 show that the dependence on T_e is relatively small at almost all the sites at which RSL observations were obtained. In addition to this, the characteristics of spatial variations of prediction are less dependent on the viscosity structure models. In particular, spatial variations of GIA results based on thin T_e model are reflective of the adoption of ice model. This is attributed to short-wavelength deformation of the Earth dominantly. Taking such property into account, we can obtain the appropriate ice load model without considering more details of the Earth's structure. Furthermore, we can reasonably explain the RSL observations accumulated to date in Antarctica using the ice models of ANT5 and IJ05, which show no melting at approximately 14.6 cal. kyr BP related to the MWP-1A event. There are essentially no RSL observations before 10 kyr BP depicted in Figs. 5 and 6, which indicates that the Antarctic contribution of MWP-1a cannot be accurately derived from the near-field RSL observations at this time. The far-field RSLs obtained in Tahiti (Deschamps et al., 2012) indicate that the amplitude of this event is approximately 14–18 m, and the GIA modelling by Bassett et al. (2005) suggested a 50% contribution from the southern hemisphere at MWP-IA. However, the total amounts of ESL since the LGM predicted by recent ice models, ANT5 and IJ05 (Fig. 2), are below approximately 20 m, corresponding to a 50–70% of the total sea level rise in Antarctica. In addition, Nakada and Lambeck (1988) suggested that minor Antarctic melting equivalent to an ESL rise of approximately 3 m occurred throughout the Holocene based on their analysis of the far-field RSLs. Additional far-field studies in Japan (Nakada et al., 1998; Okuno and Nakada, 1998; Yokoyama et al., 2012) and the Mediterranean Sea (Stocchi et al., 2009) reinforce this scenario. These studies suggest that the Antarctic ice sheet continued to melt during the last deglaciation. To estimate the Antarctic contribution of MWP-1A, we need not only RSL observations in the coastal regions but also geographical evidence of the ice retreat history in other ice-free areas in the Antarctic continent using cosmic exposure dating (e.g., Bentley et al., 2010; Yamane et al., 2011).

In this study, we discussed some of the model variations of GIA calculations using the previous ice models. These results provide useful insights for validating the plausibility of the melting models of the Antarctic ice sheet. The comparison between the GIA predictions and the field observations is constrained to the deglacial history of the Antarctic ice sheet. If effective ice models are published, we can reduce the uncertainty of interpretation of the space geodetic observations such as GPS and GRACE to more precisely estimate the effect on the Antarctic ice mass balance of recent global warming.

Acknowledgements

We thank comments from anonymous reviewer and Guest Editor Dr. Toshiaki Tsunogae. This work was partly supported by JSPS KAKENHI grant numbers 23501255, 21253001.

References

Argus, D.F., Peltier, W.R., Watkins, M., 1999. Glacial isostatic adjustment observed using very long baseline interferometry and satellite laser ranging geodesy. Journal of Geophysical Research 104, 29077–29093.

Argus, D.F., Peltier, W.R., 2010. Constraining models of postglacial rebound using space geodesy: a detailed assessment of model ICE-5G (VM2) and its relatives. Geophysical Journal International 181, 697–723.

Baroni, C., Hall, B.L., 2004. A new Holocene relative sea-level curve for Terra Nova Bay, Victoria Land, Antarctica. Journal of Quaternary Science 19, 377–396.

Bassett, S., Milne, G.A., Bentley, M., Huybrechts, P., 2007. Modelling Antarctic sea-level data to explore the possibility of a dominant Antarctic contribution to meltwater pulse IA. Quaternary Science Reviews 26, 2113–2127.

Bassett, S., Milne, G.A., Mitrovica, J.X., Clark, P.U., 2005. Ice sheet and solid earth influences on far-field sea-level histories. Science 309, 925–928.

Bentley, M., Hodgson, D., Smith, J., Cox, N., 2005. Relative sea level curves for the South Shetland Islands and Marguerite Bay, Antarctic Peninsula. Quaternary Science Reviews 24, 1203–1216.

Bentley, M.J., Fogwill, C.J., Le Brocq, A.M., Hubbard, A.L., Sugden, D.E., Dunai, T.J., Freeman, S.P.H.T., 2010. Deglacial history of the West Antarctic Ice Sheet in the Weddell Sea embayment: constraints on past ice volume change. Geology 38, 411–414.

Clark, P.U., Mitrovica, J.X., Milne, G.A., Tamisiea, M., 2002. Sea-level fingerprinting as a direct test for the source of global meltwater pulse IA. Science 295, 2438–2441.

Denton, G.H., Hughes, T.J., 1981. Last Great Ice Sheets. John Wiley & Sons, New York, 484 pp.

Deschamps, P., Durand, N., Bard, E., Hamelin, B., Camoin, G., Thomas, A.L., Henderson, G.M., Okuno, J., Yokoyama, Y., 2012. Ice-sheet collapse and sea-level rise at the Bølling warming 14,600 years ago. Nature 483, 559–564.

Dziewonski, A.M., Anderson, D.L., 1981. Preliminary reference earth model. Physics of The Earth and Planetary Interiors 25, 297–356.

Fairbanks, R., 1989. A 17,000-year glacio-eustatic sea level record: influence of glacial melting rates on the Younger Dryas event and deep-ocean circulation. Nature 342, 637–642.

Farrell, W., Clark, J.A., 1976. On postglacial sea level. Geophysical Journal of the Royal Astronomical Society 46, 647–667.

Forte, A.M., Mitrovica, J.X., 1996. New inferences of mantle viscosity from joint inversion of long wavelength mantle convection and post-glacial rebound data. Geophysical Research Letters 23, 1147–1150.

Goodwin, I.D., 1993. Holocene deglaciation, sea-level change, and the emergence of the Windmill Islands, Budd Coast, Antarctica. Quaternary Research 40, 70–80.

Hall, B.L., Henderson, G.M., Baroni, C., Kellogg, T.B., 2010. Constant Holocene Southern-Ocean ^{14}C reservoir ages and ice-shelf flow rates. Earth and Planetary Science Letters 296, 115–123.

Hanebuth, T., Stattegger, K., Grootes, P.M., 2000. Rapid flooding of the Sunda Shelf: a late-glacial sea-level record. Science 288, 1033–1035.

Ivins, E.R., James, T.S., 2005. Antarctic glacial isostatic adjustment: a new assessment. Antarctic Science 17, 541–553.

James, T.S., Ivins, E.R., 1998. Predictions of Antarctic crustal motions driven by present-day ice sheet evolution and by isostatic memory of the Last Glacial Maximum. Journal of Geophysical Research 103, 4993–5017.

Johnston, P., 1993. The effect of spatially non-uniform water loads on prediction of sea-level change. Geophysical Journal International 114, 615–634.

Kaufmann, G., Lambeck, K., 2000. Mantle dynamics, postglacial rebound and the radial viscosity profile. Physics of The Earth and Planetary Interiors 121, 301–324.

Kaufmann, G., Lambeck, K., 2002. Glacial isostatic adjustment and the radial viscosity profile from inverse modeling. Journal of Geophysical Research 107, 2280–2295.

Lambeck, K., 1993. Glacial rebound of the British Isles – I. Preliminary model results. Geophysical Journal International 115, 941–959.

Lambeck, K., Chappell, J., 2001. Sea level change through the last glacial cycle. Science 292, 679–686.

Lambeck, K., Johnston, P., Smither, C., Nakada, M., 1996. Glacial rebound of the British Isles – III. Constraints on mantle viscosity. Geophysical Journal International 125, 340–354.

Lambeck, K., Nakada, M., 1990. Late Pleistocene and Holocene sea-level change along the Australian coast. Palaeogeography, Palaeoclimatology, Palaeoecology 89, 143–176.

Lambeck, K., Purcell, A., Johnston, P., Nakada, M., Yokoyama, Y., 2003. Water-load definition in the glacio-hydro-isostatic sea-level equation. Quaternary Science Reviews 22, 309–318.

Lambeck, K., Smither, C., Johnston, P., 1998. Sea-level change, glacial rebound and mantle viscosity for northern Europe. Geophysical Journal International 134, 102–144.

Lambeck, K., Yokoyama, Y., Purcell, T., 2002. Into and out of the Last Glacial Maximum: sea-level change during Oxygen Isotope Stages 3 and 2. Quaternary Science Reviews 21, 343–360.

Lambert, A., Courtier, N., Sasagawa, G., Klopping, F., Winester, D., James, T., Liard, J., 2001. New constraints on Laurentide postglacial rebound from absolute gravity measurements. Geophysical Research Letters 28, 2109–2112.

Long, A., Roberts, D., 2003. Late Weichselian deglacial history of Disko Bugt, West Greenland, and the dynamics of the Jakobshavns Isbrae ice stream. Boreas 32, 208–226.

Milne, G.A., Davis, J., Mitrovica, J.X., Scherneck, H., 2001. Space-geodetic constraints on glacial isostatic adjustment in Fennoscandia. Science 291, 2381–2385.

Milne, G.A., Mitrovica, J.X., 1996. Postglacial sea-level change on a rotating Earth – first results from a gravitationally self-consistent sea-level equation. Geophysical Journal International 126, F13–F20.

Milne, G.A., Mitrovica, J.X., 1998a. The influence of time-dependent ocean-continent geometry on predictions of post-glacial sea level change in Australia and New Zealand. Geophysical Research Letters 25, 793–796.
Milne, G.A., Mitrovica, J.X., 1998b. Postglacial sea-level change on a rotating Earth. Geophysical Journal International 133, 1–19.
Milne, G.A., Mitrovica, J.X., 2002. Estimating past continental ice volume from sea-level data. Quaternary Science Reviews 21, 361–376.
Milne, G.A., Mitrovica, J.X., Davis, J.L., 1999. Near-field hydro-isostasy: the implementation of a revised sea-level equation. Geophysical Journal International 139, 464–482.
Mitrovica, J.X., Forte, A.M., 1997. Radial profile of mantle viscosity: results from the joint inversion of convection and postglacial rebound observables. Journal of Geophysical Research 102, 2751–2769.
Mitrovica, J.X., Forte, A.M., 2004. A new inference of mantle viscosity based upon joint inversion of convection and glacial isostatic adjustment data. Earth and Planetary Science Letters 225, 177–189.
Mitrovica, J.X., Milne, G.A., 2003. On post-glacial sea level: I. General theory. Geophysical Journal International 154, 253–267.
Mitrovica, J.X., Wahr, J., Matsuyama, I., Paulson, A., 2005. The rotational stability of an ice-age earth. Geophysical Journal International 161, 491–506.
Miura, H., Maemoku, H., Moriwaki, K., 2002. Holocene raised beach stratigraphy and sea-level history at Kizahashi Beach, Skarvsnes, Lützow-Holm Bay, Antarctica. The Royal Society of New Zealand Bulletin 35, 391–396.
Nakada, M., Kimura, R., Okuno, J., Moriwaki, K., Miura, H., Maemoku, H., 2000. Late Pleistocene and Holocene melting history of the Antarctic ice sheet derived from sea-level variations. Marine Geology 167, 85–103.
Nakada, M., Lambeck, K., 1987. Glacial rebound and relative sea-level variations: a new appraisal. Geophysical Journal of the Royal Astronomical Society 90, 171–224.
Nakada, M., Lambeck, K., 1988. The melting history of the late Pleistocene Antarctic ice sheet. Nature 333, 36–40.
Nakada, M., Lambeck, K., 1989. Late Pleistocene and Holocene sea-level change in the Australian region and mantle rheology. Geophysical Journal 96, 497–517.
Nakada, M., Lambeck, K., 1991. Late Pleistocene and Holocene sea-level change; evidence for lateral mantle viscosity structure? In: Sabadini, R., Lambeck, K., Boschi, E. (Eds.), Glacial Isostasy, Sea-level and Mantle Rheology. Kluwer Academic Publishers, Dordrecht, pp. 79–94.
Nakada, M., Okuno, J., Yokoyama, Y., Nagaoka, S., Takano, S., Maeda, Y., 1998. Mid-Holocene underwater Jomon sites along the west coast of Kyushu, Japan, hydro-isostasy and asthenospheric viscosity. The Quaternary Research 37, 315–323.
Okuno, J., Nakada, M., 1998. Rheological structure of the upper mantle inferred from the Holocene sea-level change along the West coast of Kyushu, Japan. In: Wu, P. (Ed.), Dynamics of the Ice Age Earth: A Modern Perspective. Trans Tech Publications, Switzerland, pp. 443–458.
Okuno, J., Nakada, M., 1999. Total volume and temporal variation of meltwater from last glacial maximum inferred from sea-level observations at Barbados and Tahiti. Palaeogeography, Palaeoclimatology, Palaeoecology 146, 283–293.
Okuno, J., Nakada, M., 2001. Effects of water load on geophysical signals due to glacial rebound and implications for mantle viscosity. Earth Planets Space 53, 1121–1135.
Okuno, J., Nakada, M., 2002. Contributions of ineffective ice load on sea-level and free-air gravity. Geodynamics Series 29. In: Mitrovica, J.X., Vermeersen, B. (Eds.), Ice Sheet, Sea Level and the Dynamic Earth. American Geophysical Union, pp. 177–185.
Omoto, K., 1983. The Problem and Significance of Radiocarbon Geochronology in Antarctica – Chronological Interpretation of Raised Beaches based on Levelings and Radiocarbon Datings, vol. 28. Science Reports of Tohoku University, pp. 95–148.
Peltier, W.R., 1974. The impulse response of a Maxwell Earth. Review of Geophysics and Space Physics 12, 649–669.
Peltier, W.R., 2004. Global glacial isostasy and the surface of the ice-age Earth: the ICE-5G (VM2) model and GRACE. Annual Review of Earth and Planetary Sciences 32, 111–149.
Peltier, W.R., 2005. On the hemispheric origins of meltwater pulse 1a. Quaternary Science Reviews 24, 1655–1671.
Peltier, W.R., Drummond, R., 2008. Rheological stratification of the lithosphere: a direct inference based upon the geodetically observed pattern of the glacial isostatic adjustment of the North American continent. Geophysical Research Letters 35, L16314. http://dx.doi.org/10.1029/2008GL034586.
Reimer, P.J., Baillie, M.G.L., Bard, E., Bayliss, A., Beck, J.W., Blackwell, P.G., Ramsey, C.B., Buck, C.E., Burr, G.S., Edwards, R.L., Friedrich, M., Grootes, P.M., Guilderson, T.P., Hajdas, I., Heaton, T.J., Hogg, A.G., Hughen, K.A., Kaiser, K.F., Kromer, B., McCormac, F.G., Manning, S.W., Reimer, R.W., Richards, D.A., Southon, J.R., Talamo, S., Turney, C.S.M., Van der Plicht, J., Weyhenmeyer, C.E., 2009. IntCal09 and Marine09 radiocarbon age calibration curves, 0-50,000 years CAL BP. Radiocarbon 51, 1111–1150.
Saito, F., Abe-Ouchi, A., 2010. Modelled response of the volume and thickness of the Antarctic ice sheet to the advance of the grounded area. Annals of Glaciology 51, 41–48.
Spada, G., Stocchi, P., 2007. SELEN: a Fortran 90 program for solving the "sea-level equation". Computers & Geosciences 33, 538–562.
Steffen, H., Kaufmann, G., 2005. Glacial isostatic adjustment of Scandinavia and northwestern Europe and the radial viscosity structure of the Earth's mantle. Geophysical Journal International 163, 801–812.
Stocchi, P., Colleoni, F., Spada, G., 2009. Bounds on the time-history and Holocene mass budget of Antarctica from sea-level records in SE Tunisia. Pure and Applied Geophysics 166, 1319–1341.
Stuiver, M., Pearson, G.W., Braziunas, T., 1986. Radiocarbon age calibration of marine samples back to 9000 cal.yr BP. Radiocarbon 28, 980–1021.
Tushingham, A.M., Peltier, W.R., 1991. Ice-3G: a new global model of Late Pleistocene deglaciation based upon geophysical predictions of post-glacial relative sea level change. Journal of Geophysical Research 96, 4497–4523.
Velicogna, I., Wahr, J., 2002. A method for separating Antarctic postglacial rebound and ice mass balance using future ICES at Geoscience Laser Altimeter System, Gravity Recovery and Climate Experiment, and GPS satellite data. Journal of Geophysical Research 107, 2263. http://dx.doi.org/10.1029/2001JB000708.
Whitehouse, P.L., Bentley, M.J., Le Brocq, A.M., 2012a. A deglacial model for Antarctica: geological constraints and glaciological modelling as a basis for a new model of Antarctic glacial isostatic adjustment. Quaternary Science Reviews 32, 1–24.
Whitehouse, P.L., Bentley, M.J., Milne, G.A., King, M.A., Thomas, I.D., 2012b. A new glacial isostatic adjustment model for Antarctica: calibrated and tested using observations of relative sea-level change and present-day uplift rates. Geophysical Journal International. http://dx.doi.org/10.1111/j.1365–246X.2012.05557.x.
Yamane, M., Yokoyama, Y., Miura, H., Maemoku, H., Iwasaki, S., Matsuzaki, H., 2011. The last deglacial history of Lützow-Holm Bay, East Antarctica. Journal of Quaternary Science 26, 3–6.
Yokoyama, Y., Lambeck, K., De Deckker, P., Johnston, P., Fifield, L.K., 2000. Timing of the Last Glacial Maximum from observed sea-level minima. Nature 406, 713–716.
Yokoyama, Y., Okuno, J., Miyairi, Y., Obrachta, S., Demboya, N., Makino, Y., Kawahata, H., 2012. Holocene sea-level change and Antarctic melting history derived from geological observations and geophysical modeling along the Shimokita Peninsula, northern Japan. Geophysical Research Letters 39, L13502. http://dx.doi.org/10.1029/2012GL051983.
Zwartz, D., Bird, M., Stone, J., Lambeck, K., 1998. Holocene sea-level change and ice-sheet history in the Vestfold Hills, East Antarctica. Earth and Planetary Science Letters 155, 131–145.